Proceedings of the Seventh International Conference on
Railway Technology: Research, Development and Maintenance
Edited by: J. Pombo
Civil-Comp Conferences, Volume 15, Paper 5.14
Civil-Comp Press, Edinburgh, United Kingdom, 2026
ISSN: 2753-3239, doi: 10.4203/ccc.15.5.14

An Interoperable Railway Vehicle Model for Crosswind Safety Assessment

L. Favaro and G. Tomasini

Department of Mechanical Engineering, Politecnico di Milano, Italy

Abstract

As high-speed rail networks grow, ensuring interoperability between different lines and vehicles has become a primary requirement, particularly in crosswind assessment where line-level analyses remain strongly dependent on the specific vehicles adopted, making the definition of a common reference particularly useful. To address this need, this work presents a methodology to define an equivalent "interoperable" vehicle model, intended as a TSI-consistent reference whose Characteristic Wind Curves (CWCs) directly reproduce the regulatory Reference CWCs under the operating conditions prescribed by the standards. Formulated as an inverse calibration task, the problem is solved through a two-stage Bayesian Optimisation (BO) framework constrained by realistic data from a representative fleet of European high-speed trains. Operating over an input space comprising both multibody and standard-derived wind tunnel aerodynamic coefficients, the BO jointly adjusts these properties, followed by a final refinement based on a reparameterisation strategy for the aerodynamic curves. Applied to a high-speed baseline train, this framework validates a robust approach to define a standardized reference vehicle model, offering a consistent vehicle representation of TSI regulatory limits and ultimately supporting railway interoperability.

Keywords: crosswind stability, characteristic wind curves, railway interoperability, railway vehicle dynamics, inverse model calibration, bayesian optimisation

1 Introduction

Over the past decades, driven by the ongoing development of high-speed vehicles and the expanding high-speed railway networks, crosswind safety has gained significant and continuous attention from the international railway community, further reinforced by the increasing operating speeds and the widespread adoption of distributed-power solutions, which make aerodynamic effects more critical for running stability and ultimately increase vehicle sensitivity to overturning.

In this scenario, the joint effort of the various actors involved, including academia and railway operators, has gradually led to the development of a unified framework for crosswind assessment, comprising common standards and procedures. This framework is mainly embodied in the TSI - namely Technical Specifications for Interoperability standards [1] - aimed at supporting the interoperability and harmonisation of the railway system and refers to EN 14067-6: 2018 [2] for the technical aspects related to the safety of train operations under crosswind conditions.

1.1 Crosswind Safety Regulatory Framework

Building on this framework, crosswind risk is managed through a coordinated approach involving both the rolling stock and infrastructure subsystems. On the rolling stock side, the LOC&PAS TSI [3] requires the evaluation of the Characteristic Wind Curves (CWCs) for train's most wind-sensitive vehicle, in accordance with EN 14067-6. These curves define the critical gust wind speed associated with a prescribed safety limit, namely the 90% wheel-unloading criterion for the windward bogie, regarded as precursor to vehicle overturning.

Following TSI guidelines, the safety proof is performed through time-dependent vehicles multibody dynamics (MBD) simulations, with aerodynamic loads modelled according to the quasi-steady theory - using aerodynamic force and moment coefficients experimentally derived through wind-tunnel testing in the Single Track Ballast and Rail (STBR) reference configuration - applied to the MBD model under the standard "Chinese hat" deterministic wind gust scenario.

Vehicle compliance is finally verified by comparing the train CWCs with the corresponding Reference Characteristic Wind Curves (RCWCs), which define the minimum acceptable crosswind performance for the train class under consideration.

On the infrastructure side - as per the INF TSI [4] - it is the responsibility of the Infrastructure Manager to identify the sections of a line that may be exposed to severe wind conditions and, where necessary, to reduce the associated operational risk. This issue has been extensively addressed in previous studies at the European level [5, 6], which provided guidance on wind exposure assessment and on the demonstration of operational safety under crosswind conditions.

In this context, the overturning risk is regarded as the combined probability of severe wind gusts occurring at a given site and the train reaching its crosswind safety limit while running through the exposed section. Therefore, the assessment of a railway line requires the information about local wind exposure to be combined with the line speed profile and the relevant RCWCs, in order to reliably identify the locations where admissible safety limits may be exceeded [7, 8].

1.2 Interoperability Requirements for Crosswind Assessment

However, under this framework, line-level crosswind assessment remains inherently linked to the characteristics of the specific vehicle considered for the analysis. Indeed, whenever new lines are designed, existing ones reassessed or additional crosswind mitigation measures introduced, the assessment must be reconsidered with respect to the trains expected to operate on the line: this is particularly relevant for new railways, where higher design speeds may be combined with new topographical layouts locally exposed to severe wind conditions. This naturally brings the line-oriented assessment of crosswind safety into the broader context of railway interoperability.

In this regard, the INF TSI provides a key indication by stating that a line can be considered ”interoperable” from a crosswind perspective if safety is ensured for a reference train running under the most critical operational conditions. This requirement makes the availability of a common reference - against which the crosswind safety of the infrastructure can be evaluated - particularly valuable, as it would ensure interoperability while avoiding costly and time-consuming reanalyses for every new fleet.

In fact, if a line is assessed against a standard reference performance consistent with regulatory limits, any train whose CWCs comply with the corresponding RCWCs can be considered compatible with that infrastructure from the crosswind safety point of view; the same reasoning holds for line-side mitigation strategies, as evaluating their validity on a common reference basis ensures they are inherently effective for all vehicles compliant with the TSI requirements. In order to characterise the line independently from the specific operating railway vehicle considered in the assessment, these considerations naturally call for the definition of an “interoperable train” model.

1.3 Proposed Approach: Interoperable Vehicle Modelling

To address this need, this work proposes the definition of an equivalent interoperable vehicle model for crosswind assessment purposes. The objective is to develop a simulation model whose overturning thresholds directly reproduce the safety limits prescribed by the regulations. Specifically, the model is calibrated so that its CWCs coincide with - or lie slightly below, for conservativeness - the RCWCs defined by the TSI for high-speed trains operating between 250 and 360 km/h, covering all speeds and operational conditions required for compliance.

According to the developed methodology, the model is derived starting from a validated baseline of an existing high-speed vehicle, chosen for its nominal proximity to the target crosswind performance and supported by reliable aerodynamic data extracted directly from the reference regulatory documentation [2]. An inverse calibration procedure is then applied, systematically adjusting the relevant MBD and aerodynamic parameters across a prescribed admissible design space, until the simulated CWCs converge toward the target regulatory curves (i.e. the objective RCWCs).

Once calibrated, the model provides a physical and numerical standardised representation of the regulatory crosswind limit and can therefore serve as the reference vehicle in infrastructure-side assessments or in the evaluation of line-side mitigation strategies: a line verified against this model can hence be assessed at the same safety level required by the TSI framework and any mitigation measure validated on this basis can be considered effective for all TSI-compliant rolling stock, making the proposed interoperable train a consistent and robust reference for crosswind assessment.

2 Methods

The definition of an interoperable vehicle model requires the regulatory crosswind requirements to be expressed in a form suitable for numerical calibration. In this work, this is done by reformulating the standard crosswind compliance assessment as an inverse problem, in which the RCWCs impose the target response and the model parameters are adjusted accordingly. The following methodology describes this reformulation and its implementation within the adopted simulation framework.

The baseline simulation model used in this work is a 3D multibody representation of the leading vehicle of a high-speed trainset modelled with A.D.Tre.S, a multibody code developed by the Mechanical Engineering Department of Politecnico di Milano. Consistently with the TSI requirements, the model focuses on a single vehicle representative of the most wind-sensitive unit of the train.

2.1 TSI Operating Conditions for Crosswind Compliance

According to [2], crosswind safety assessment is based on a finite set of operating conditions to be verified for compliance. These conditions are defined by specific combinations of train speed, wind angle to the track and uncompensated lateral acceleration and identify the CWC entries that must be verified for straight and curved-track operation; the corresponding RCWCs provide the reference wind speed values against which vehicle performance is compared. In this study, the inverse calibration problem is formulated starting from the same operating points required for TSI compliance.

The actual definition of this domain is guided by several practical considerations. First, only the scenarios for which the TSI provides the corresponding RCWCs are retained, since these are the curves defining the regulatory targets to be matched. Secondly, although the baseline high-speed vehicle has a maximum speed of 360 km/h, the interoperable model is intended for operation on the Italian high-speed network, where the maximum allowable speed is limited to 300 km/h, justifying a further reduction of the main calibration dataset.

However, including all remaining regulatory combinations within a single objective function would still result in an excessively complex formulation of the problem. To keep the computational effort reasonable while preserving the physical consistency of the model, the actual operating conditions are divided into two distinct sets of points:

- **Calibration points:** these are defined as mandatory targets and represent the operating conditions directly embedded into the calibration problem. They are selected to ensure sufficient dynamic coverage and to prevent an unphysical over-adaptation of vehicle's parameters to a few isolated conditions. Although they mostly coincide with the scenarios explicitly required by the TSI tables for compliance, additional specific curved track conditions at 330 and 350 km/h are included, too: since curving CWCs represent the most critical ones to match, targeting these extra points ensures a robust and more accurate result.

- **Validation points:** these are implemented to assess the global robustness of the model in operational conditions unseen by the calibration procedure. Extending up to 360 km/h, they are used to verify a posteriori that the resulting model maintains its physical consistency and behavioural accuracy across the entire spectrum of operational conditions it is expected to work in. The resulting selection is reported in Table 1, yielding a final reduced but representative set of target conditions.

a_{nc}	β_w	Train speed (km/h)																
		160	180	200	220	240	250	260	270	280	290	300	310	320	330	340	350	360
0 m/s^2	90°	**V***	**V***	**V***	**V***	**V***	**V**	**C***	**V**	**C***	**V**	**C***	**V**	**V**	**V**	**V**	**V**	**V**
	80°						**V**	**V**	**V**	**V**	**V**	**C***	**V**	**V**	**V**	**V**	**V**	**V**
	60°						**V**	**V**	**V**	**V**	**V**	**C***	**V**	**V**	**V**	**V**	**V**	**V**
	40°						**V**	**V**	**V**	**V**	**V**	**C***	**V**	**V**	**V**	**V**	**V**	**V**
0.5 m/s^2	90°						**V**	**C***	**V**	**C***	**V**	**C***	**V**	**V**	**C**	**V**	**C**	**V**
1.0 m/s^2	90°						**V**	**C***	**V**	**C***	**V**	**C***	**V**	**V**	**C**	**V**	**C**	**V**

Table 1: Form of the CWC table for non-tilting passenger vehicles and locomotives, adapted from [2]. Red cells indicate calibration points (C), while blue cells indicate validation points (V). The asterisks mark the minimum entries required by the standard for crosswind compliance.

2.2 Inverse Calibration as a Bayesian Optimization Problem

As established in the previous sections, TSI crosswind requirements have been translated into a discrete set of target conditions that are directly interpretable by the MBD simulation model. Since the primary objective of the calibration is to adjust vehicle parameters so that the model output matches the target RCWCs - hence minimizing the discrepancy between a model response and a reference objective - the calibration can be naturally formulated as a mathematical optimization procedure.

This however requires running several time-dependent MBD simulations for each operational scenario, making the objective function both expensive to evaluate and not available in closed form. Given these characteristics and the need to explore a multidimensional space efficiently, Bayesian Optimization (BO) emerges as a natural numerical strategy to solve the problem: indeed, by building a probabilistic surrogate model of the objective function, it systematically guides the search toward the TSI-calibrated configuration while keeping the number of simulations to a minimum.

To drive the BO loop, a formal objective function must be defined by integrating the regulatory requirements described in Section 2.1. These requirements define a multidimensional target hyperplane, which represents the discrete set of overturning conditions that the calibrated vehicle model must satisfy simultaneously. For each operating point on this hyperplane, the MBD model is simulated by imposing the corresponding operational inputs, namely V_{train}, β_{wind} and a_{nc}. Concurrently, the regulatory information from the RCWCs is converted into a deterministic aerodynamic forcing by prescribing a specific mean wind speed: this velocity is selected such that, after conversion, it corresponds precisely to the critical gust wind speed identified by the TSI as the overturning threshold for that specific scenario.

Under these conditions, vehicle response is evaluated through the wheel unloading criterion, using $\Delta Q/Q_0$ as the primary output $y(\mathbf{x}_k)$ of the simulation, given a candidate input configuration $\mathbf{x}$. For a perfectly calibrated model, the applied forcing will drive the vehicle exactly to its regulatory safety limit, resulting in a maximum wheel unloading equal to the target threshold $\bar{y}_k = 0.9$, $\forall k$ across all M calibration scenarios.

2.3 Input Space and Design Variables

Once the calibration problem is set, the design space must be defined by identifying the key parameters to be modified and establishing their respective variation boundaries.

The initial candidate set of design variables is chosen to include a comprehensive selection of the primary dynamic MBD properties (i.e. masses, moments of inertia, suspension stiffness, damping coefficients and the vertical z-coordinates of the centres of mass for both the car body and the bogies) as well as non-linear characteristics governing the bumpstop stiffness curve; additionally, the six aerodynamic coefficients are globally modified by means of scaling factors applied to the whole curve.

It is important to note that, with the sole exception of the vertical positions of the centres of mass, the overall layout and geometry of the vehicle are kept unaltered: this choice ensures that the procedure acts as a dynamic and aerodynamic tuning of an existing vehicle architecture rather than a structural redesign of the train.

In order to define suitable variability intervals for the candidate parameters, different bounding strategies are combined. For the dynamic parameters of the multibody model, a "reference-fleet" strategy is adopted: specifically, the minimum and maximum values observed across a reference fleet of three representative European high-speed trains are used as the absolute bounds (this represents a more constrained approach where the boundaries are dictated by realistic vehicle data).

However, a specific exception is introduced for the combination of car body mass and vertical secondary suspension stiffness. Since the three fleet trains feature highly similar mass values, a purely fleet-based approach would artificially restrict the mass parameter, preventing the optimization from exploiting its high importance shown by the sensitivity analysis. Consequently, a wider $\pm 15\%$ percentage interval around the nominal value is used for the mass. To keep the vertical dynamics physically consistent, a domain constraint is applied to this combination to maintain the resulting car body vertical frequency between 0.75 Hz and 1.40 Hz. This frequency range is also dictated by the absence of an anti-roll bar in the baseline train configuration. Table 2 shows the tentative initial space and the employed ranges for the two strategies.

Parameter		Reference Fleet			Percentages
		Train 1*	**Train 2**	**Train 3**	**Range**
Aerodynamic Coefficients $C_{F_x}, C_{F_y}, C_{F_z}, C_{M_x}, C_{M_y}, C_{M_z}$		1	–	–	±40%
Bumpstop Stiffness Curve		1	–	–	±25%
Multibody Dynamics Variables	Car body Mass M_{c} [kg]	54 840	54 244	53 500	±15%
	Car body CG Height from Rail Level h_{c} [m]	1.5000	1.7500	1.6986	
	Car body Roll Moment of Inertia $I_{x_{\mathrm{c}}}$ [kg · m^2]	65 200	58 783	70 000	–
	Car body Pitch Moment of Inertia $I_{y_{\mathrm{c}}}$ [kg · m^2]	1 170 000	1 118 055	2 621 500	
	Car body Yaw Moment of Inertia $I_{z_{\mathrm{c}}}$ [kg · m^2]	1 160 000	1 098 441	2 621 500	
	Bogie Mass M_{b} [kg]	3 150	2 382	4 844	
	Bogie Roll Moment of Inertia $I_{x_{\mathrm{b}}}$ [kg · m^2]	2 420	1 446	5 942	
	Bogie Pitch Moment of Inertia $I_{y_{\mathrm{b}}}$ [kg · m^2]	5 168	1 449	2 439	
	Bogie Yaw Moment of Inertia $I_{z_{\mathrm{b}}}$ [kg · m^2]	7 293	3 545	4 031	
	Bogie CG Height from Rail Level h_{b} [m]	0.6500	0.6500	0.5763	
	Primary Vertical Stiffness (per bogie) $k_{\mathrm{v},1}$ [N/m]	9 680 000	4 880 000	4 800 000	
	Primary Vertical Damping $r_{\mathrm{v},1}$ [N · s/m]	58 860	40 000	40 000	
	Secondary Vertical Stiffness (per bogie) $k_{\mathrm{v},2}$ [N/m]	1 790 000	2 452 000	700 000	
	Secondary Vertical Damping (per bogie) $r_{\mathrm{v},2}$ [N · s/m]	119 500	120 000	40 000	
	Secondary Lateral Stiffness (per bogie) $k_{\mathrm{o},2}$ [N/m]	466 000	612 000	200 000	
	Secondary Lateral Damping $r_{\mathrm{o},2}$ [N · s/m]	40 221	30 000	30 000	
	Car body-Bogie Yaw Damping r_{s} [N · s/m]	343 000	343 000	420 000	

Table 2: Candidate parameter set with nominal values and admissible ranges. Aerodynamic and Bumpstop variables are defined as multiplicative factors applied to the baseline curves, hence their nominal value is 1.

However, the initial design space containing all candidate parameters is too wide to be handled directly by the Gaussian Process employed in the BO; furthermore, not all selected variables have the same impact on the wheel unloading index. To reduce the dimensionality of the problem, a factor screening step is performed using the Morris One-at-a-Time (MOAT) method, allowing for effective factor fixing, i.e. the identification uninfluential parameters that can be safely locked at their nominal values without any significant loss of accuracy in the model response [9]. The resulting parameters define the global design domain, denoted in the following as $\mathcal{D}$.

2.4 Two-Step Exploration-Refinement Bayesian Optimization

The calibration of the model requires managing several design variables to simultaneously match a large set of target conditions. Because the underlying vehicle dynamics and the resulting cost function are highly complex and non-linear, decoupling the mutual effects of the parameters is inherently difficult. To overcome these difficulties and systematically guide the convergence, the calibration is structured as a two-step BO strategy, split into an ”exploratory” phase and a localized ”refinement” phase.

This separation is directly dictated by the intrinsic physical differences between mechanical and aerodynamic parameters. On one hand, MBD variables govern the baseline dynamic behaviour of the vehicle, inevitably scaling train’s crosswind resistance across the entire operational envelope. Conversely, the quasi-steady aerodynamic formulation naturally allows for localized adjustments: indeed, because the relative velocity construction links each operating condition to a specific wind incidence angle, different regions of the aerodynamic curves are ”activated” depending on the running scenario. Consequently, the BO can modify distinct zones of the curves to adjust specific portions of the CWCs, effectively decoupling the effects.

Based on these considerations, the first BO step acts as an exploratory phase, with the aim of adjusting the global mechanical parameters to bring the baseline CWCs closer to the targets. In order to let the algorithm explore the space freely, strict regulatory limits (i.e. CWCs above RCWCs) are relaxed into soft penalties. Accordingly, a comprehensive cost function $J(\mathbf{x})$ is structured as a Mean Squared Error (MSE), augmented with penalty terms to manage local discrepancies and unfeasible results

$$J(\mathbf{x}) = \frac{1}{M}\sum_{k=1}^{M}\left[(y(\mathbf{x}_k)-\bar{y}_k)^2 + \lambda_k P_k^{(1)}(\mathbf{x}_k) + \theta_k P_k^{(2)}(\mathbf{x}_k)\right] \tag{1}$$

The term $P_k^{(1)}(\mathbf{x}_k)$, weighted by λ_k, controls the maximum local error across the calibration scenarios, preventing the algorithm from reducing the global average discrepancy at the expense of critical individual conditions. Conversely, $P_k^{(2)}(\mathbf{x}_k)$, weighted by θ_k, penalizes unfeasible vehicle configurations, ensuring that the calibrated model response remains at or slightly below the target RCWC threshold. The primary outcome of this exploratory step is the optimal parameter vector $\mathbf{x}^*$, obtained by minimizing the cost function over the global domain:

$$\mathbf{x}^*_{\text{expl}} = \arg\min_{\mathbf{x}\in\mathcal{D}} J(\mathbf{x}) \tag{2}$$

Although $\mathbf{x}^*_{\text{expl}}$ brings the baseline curves significantly closer to the targets, it does not guarantee full regulatory compliance across all individual conditions. To enforce the constraints, the process shifts to the second stage: in this phase, all mechanical parameters are frozen at the values found in $\mathbf{x}^*_{\text{expl}}$ and the BO operates within a restricted aerodynamic domain $\mathcal{A}$. To exploit the aforementioned ”aerodynamic decoupling”, coefficient curves are reparameterised by dividing them into three distinct β_{w} regions.

Under this reparameterisation, the coefficients vary independently across two distinct ranges: from 0 to 15 deg and from 15 deg onwards. Specifically, a cubic smoothing spline reconstructs the updated curve by tracking the new target profile in the first region, while blending smoothly through a transition zone to connect the two regions at higher angles. This reconstruction process is governed by two main constraints:

- The cumulative pointwise percentage variation between the final refined coefficients and the original baseline must not exceed thevalue defined in Table 2. This ensures that the combined effect of both BO stages respects the boundaries originally established during the definition of $\mathcal{D}$;
- The global topology of the curves must be preserved, in order to maintain the physical validity of the aerodynamic characteristics of the vehicle and to prevent over-adaptation to individual operating conditions. An example of the developed reparameterisation strategy is shown in Fig. 1.

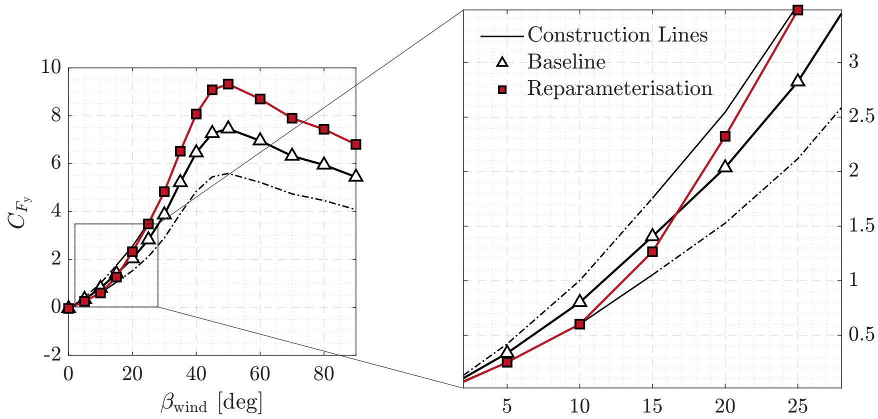

Figure 1: Example of aerodynamic curve reparameterisation. The modified curve (red) tracks the black construction lines starting from BO1 result (circles).

At this stage, the BO formulation is modified by replacing the soft penalty terms with explicit hard constraints. As a result, the objective reduces to a pure MSE (i.e. $J(\mathbf{x})$ is evaluated with $\lambda_k = \theta_k = 0$). The refinement BO problem therefore states

$$\mathbf{x}^*_{\text{ref}} = \arg\min_{\mathbf{x}\in\mathcal{A}} J(\mathbf{x}) \quad \text{s.t.} \quad c(\mathbf{x}) \leq 0 \tag{3}$$

3 Results

This section presents the outcomes of the proposed two-stage calibration methodology, evaluating the performance of both the global unconstrained optimization (BO1) and the subsequent aerodynamic refinement phase (BO2). Firstly, parameter screening via the Morris method was performed on a representative straight track ($\beta_{\text{wind}} = 90°$) condition to evaluate the 24 initial candidate variables. Table 3 below reports the ranked Elementary Effects in terms of the global sensitivity index μ^*, i.e. the Modified Mean of the Elementary Effects (EEs) [9]: six parameters with negligible impact on the wheel-unloading response were fixed at their nominal values, hence reducing the effective input space $\mathcal{D}$ for the subsequent BO1 to a final subset of 17 variables.

Parameter	μ^*	**Parameter**	μ^*	**Parameter**	μ^*	**Parameter**	μ^*
C_{F_x}	$2.5\cdot10^{-3}$	δ_b	$4.0\cdot10^{-3}$	M_b	$4.7\cdot10^{-2}$	$r_{v,1}$	$7.9\cdot10^{-4}$
C_{F_y}	$2.1\cdot10^{-2}$	M_c	$2.0\cdot10^{-2}$	I_{x_b}	$1.1\cdot10^{-3}$	$k_{v,2}$	$2.6\cdot10^{-2}$
C_{F_z}	$5.7\cdot10^{-2}$	h_c	$4.3\cdot10^{-2}$	I_{y_b}	$1.2\cdot10^{-6}$	$r_{v,2}$	$1.1\cdot10^{-2}$
C_{M_x}	$2.3\cdot10^{-1}$	I_{x_c}	$3.8\cdot10^{-3}$	I_{z_b}	$1.4\cdot10^{-4}$	$k_{o,2}$	$9.4\cdot10^{-3}$
C_{M_y}	$1.6\cdot10^{-3}$	I_{y_c}	$2.0\cdot10^{-4}$	h_b	$1.8\cdot10^{-2}$	$r_{o,2}$	$4.0\cdot10^{-4}$
C_{M_z}	$3.0\cdot10^{-2}$	I_{z_c}	$5.5\cdot10^{-3}$	$k_{v,1}$	$4.6\cdot10^{-3}$	r_s	$4.2\cdot10^{-4}$

Table 3: MOAT sensitivity indices ranked by μ^*. Blue cells identify the parameters retained for the calibration. For this case, $r_{v,2}$ was fixed at its nominal value.

Following the global SA, the BO framework was applied to calibrate the equivalent vehicle model. The final outcome of the process is reported in Figure 2: nominal CWCs (i.e. the starting point of the procedure) are shown together with the resulting curves after each BO-stage and compared to the corresponding RCWCs. Results are grouped according to the six main operating conditions described in Table 1: four straight-track cases with decreasing wind angles ($\beta_{\text{wind}} = 90, 80, 60, 40$ deg) and two curved-track cases with $a_{\text{nc}} = 0.5$ m/s^2 and 1.0 m/s^2.

For the straight-track case at $\beta_{\text{wind}} = 90°$, the calibrated model shows good agreement with the target RCWCs over the full speed range, including the low-speed region starting from 160 km/h (which was not directly used for calibration), with the residual discrepancy remaining within approximately 1 m/s. As the wind angle decreases, the calibrated curves consistently follow the target trend, although the distance from the RCWCs becomes more evident, particularly for $\beta_{\text{wind}} = 60°$ and 40°: this specific behaviour is consistent with both the initial nominal response - which placed itself already significantly above the target curves for these angles - and the adopted calibration strategy, where these specific conditions were controlled through only a single central point at 300 km/h, with remaining points retained only for the validation phase. While this choice was consistent with the specific compliance criteria prescribed by the TSI standards, the distance from the reference curves could be further reduced by distributing additional calibration points along the velocity profile.

As regards the curved-track conditions, they represent the most demanding cases for the optimization. Since their CWCs proved to be inherently more difficult to shift towards the reference limits, the calibration process prioritised their reduction, accepting a limited loss of accuracy in the less critical straight-track scenarios. Indeed, for the $a_{\text{nc}} = 0.5$ m/s^2 case, the final curve closely follows the target RCWC, remaining distributed just below the prescribed limit. For $a_{\text{nc}} = 1.0$ m/s^2, the agreement is satisfactory within the speed range relevant for compliance on the considered infrastructure (up to 300 km/h). Above this value, the CWC rises slightly above the reference curve; however, this does not affect the intended application, due to the aforementioned limit for the Italian high-speed lines of 300 km/h.

As visible from Figure 2, the solutions obtained from the two BO-stages are very similar (in the tangent track scenarios the respective CWCs are nearly overlapping); however, the local refinement performed in the second stage is essential to achieve compliance. Indeed, the BO1-solution severely violates the target thresholds in the curved track case at $a_{\text{nc}} = 1.0$ m/s^2, which would make the vehicle model unacceptable. A similar behaviour occurs for isolated points at higher speeds in the $a_{\text{nc}} = 0.5$ m/s^2 and straight-track, 60 deg conditions. The BO2-stage resolves these specific local violations by slightly sacrificing the performance in the less critical tangent track conditions, ensuring a fully compliant final model over the range of interest.

Overall, the results demonstrate that the proposed methodology achieves satisfactory outcomes with a limited number of calibration points. Crucially, the interoperable vehicle model preserves its global ”physical” characteristics without experiencing behavioural distortions: the underlying dynamics is indeed correctly maintained, allowing for validation of the model even outside the calibration domain. Although the framework allows for additional calibration points, results prove that a well-selected subset of TSI conditions is sufficient to generate a robust reference model. This is particularly evident in the low-speed region of the $\beta_{\text{wind}} = 90°$ case and for the lower-angle straight-track conditions, where a single calibration point was sufficient to preserve the global shape of the CWCs (although with a larger distance from the target). To illustrate the parameter variations that led to these results, Table 4 details the final, complete dataset of the multibody model.

Parameter	**Value**	**Parameter**	**Value**
Car body Mass M_c [kg]	51 955	Bogie Mass M_b [kg]	2 611
Car body CG Height h_c [m]	1.7000	Bogie CG Height h_b [m]	0.6500
Car body Roll Inertia I_{x_c} [kg m^2]	59 238	Bogie Roll Inertia I_{x_b} [kg m^2]	1 839
Car body Pitch Inertia I_{y_c} [kg m^2]	1 170 000	Bogie Pitch Inertia I_{y_b} [kg m^2]	5 168
Car body Yaw Inertia I_{z_c} [kg m^2]	1 764 377	Bogie Yaw Inertia I_{z_b} [kg m^2]	7 293
Primary Vertical Stiffness (pb) $k_{v,1}$ [N/m]	5 456 175	Primary Vertical Damping (pb) $r_{v,1}$ [N s/m]	58 860
Secondary Vertical Stiffness (pb) $k_{v,2}$ [N/m]	718 243	Secondary Vertical Damping (pb) $r_{v,2}$ [N s/m]	119 500
Secondary Lateral Stiffness $k_{o,2}$ [N/m]	224 858	Secondary Lateral Damping $r_{o,2}$ [N s/m]	40 221
Car body-Bogie Yaw Damping r_s [N s/m]	343 000	Vehicle Length [m]	20.48

Table 4: Final MBD parameter values adopted for the calibrated vehicle model.

Figure 3 reports the aerodynamic coefficients before and after the two BO stages. Due to their lower influence on the crosswind stability response, C_{F_x} and C_{M_y} are adjusted only during the exploratory phase and are then kept fixed at their BO1-values during the refinement stage. Conversely, the reparametesized coefficients are allowed to vary locally in the second phase to improve the matching of the target curves. Among them, only C_{F_y} fully exploits its prescribed variability range (the final solution is also associated with a adjustment of the car body CG-height), while the remaining aerodynamic coefficients undergo only limited modifications with respect to their baseline values, thus indicating that the target CWCs could be successfully matched mainly through localised parameter adjustments.

4 Conclusions and Contributions

A methodology for the definition of an interoperable railway vehicle model for crosswind assessment was proposed. Starting from a baseline vehicle model, the calibration demonstrated that a reference model exhibiting the desired CWC-specifications can be successfully constructed using a relatively small and well-selected set of parameters, whose values do not deviate excessively from those of high-speed trains currently in operation. The performed case study showed that the calibrated model exhibits satisfactory performance across all considered scenarios, particularly within the speed range of primary regulatory relevance for the Italian high-speed network. The strength of the approach lies in its ability to recover the desired crosswind performance starting from a physically meaningful and constrained parameter set: by anchoring the calibration within realistic bounds derived from existing high-speed trains, the resulting reference model retains full physical consistency while accurately reproducing the regulatory targets, generalising reliably beyond the calibration domain.

Future studies will focus on extending and validating the model across a wider range of operational conditions, as well as introducing additional constraints within the optimization phase to further enhance its robustness and generalisability. Ultimately, the proposed interoperable vehicle model provides a robust representation of the TSI crosswind safety limits, enabling its direct use as a standardized reference for infrastructure-level risk assessments and for the validation of line-side mitigation strategies: any measure verified against this model can be considered effective for all TSI-compliant rolling stock, substantially supporting railway interoperability without requiring vehicle-specific reanalyses. To this end, the model will be deployed in the crosswind risk analysis of reference high-speed railway lines, where infrastructure-side wind exposure data will be combined with the dynamics of the calibrated vehicle to produce line-level risk assessments. The results will then be compared against those previously obtained using fleet-specific trains on the same lines, allowing a direct evaluation of the interoperable model's predictive consistency and ultimately validating its role as a reliable reference for crosswind assessment studies on real infrastructure.

References

[1] TSI, 2014. Technical specification for interoperability relating to the rolling stock-locomotives and passenger rolling stock subsystem of the rail system in the European Union. Off. J. Eur. Union L 356, 228-393.

[2] EN 14067-6, 2018. Railway Applications - Aerodynamics, Part 6: Requirements and Test Procedures for Cross Wind Assessment. CEN, Brussels, 2018.

[3] Commission Regulation n° 1302/2014 of 18 Nov 2014 on the Technical Specification for Interoperability relating to the "Rolling Stock - Locomotives and

Passenger Rolling Stock” Subsystem of the Rail System in the European Union. Off. J. Eur. Union L 356.

[4] Commission regulation n° 1299/2014 of 18 Nov 2014 on the Technical Specification for Interoperability relating to the ”Infrastructure” Subsystem of the Rail System in the European Union. Off. J. Eur. Union L 356.

[5] UIC Rail System Department, 2021. SAFIRST - Vehicle Assessment Technical Report. International Union of Railways (UIC), July 2021.

[6] UIC Rail System Department, 2021. SAFIRST - Application of Reference Characteristic Wind Curves. International Union of Railways (UIC), Dec 2021.

[7] G. Diana, M. Burlando, F. Cheli, A. Freda, C.F. Ratto, D. Rocchi, G. Solari, M. Testa, G. Tomasini, ”A new methodology to perform the risk analysis of cross wind on high speed lines”. Proceedings of the 8$^{\text{th}}$ World Congress on Railway Research, Seoul, Korea, 18-22 May 2008.

[8] G. Crespi, S. Giappino, G. Tomasini, ”Anemometer-Based Approach for Evaluating Overturning Risk Along Railway Lines”. Proceedings of the Sixth International Conference on Railway Technology: Research, Development and Maintenance, Prague, Czech Republic, 1-5 Sept. 2024.

[9] A. Saltelli, M. Ratto, T. Andres, F. Campolongo, J. Cariboni, D. Gatelli, M. Saisana, S. Tarantola, Global Sensitivity Analysis. Wiley, NJ, USA, 2008.

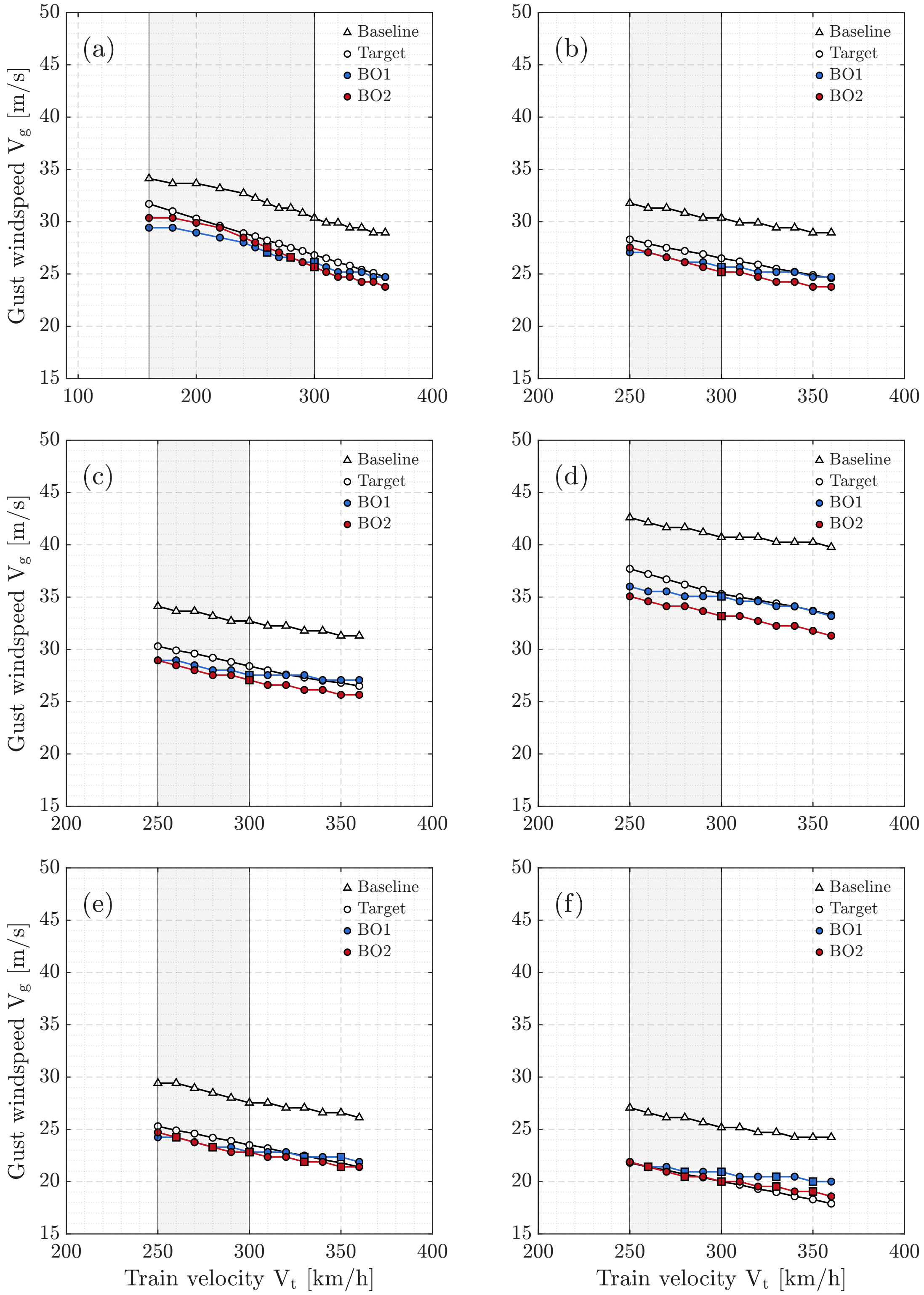

Figure 2: RCWCs compared with nominal, BO1 and BO2 CWCs. Grey areas denote TSI-required ranges; square/circular markers indicate calibration/validation points. (a)-(d) Straight-track, $\beta_w = 90°, 80°, 60°, 40°$; (e)-(f) curve, $a_{nc} = 0.5, 1.0\,\mathrm{m/s^2}$.

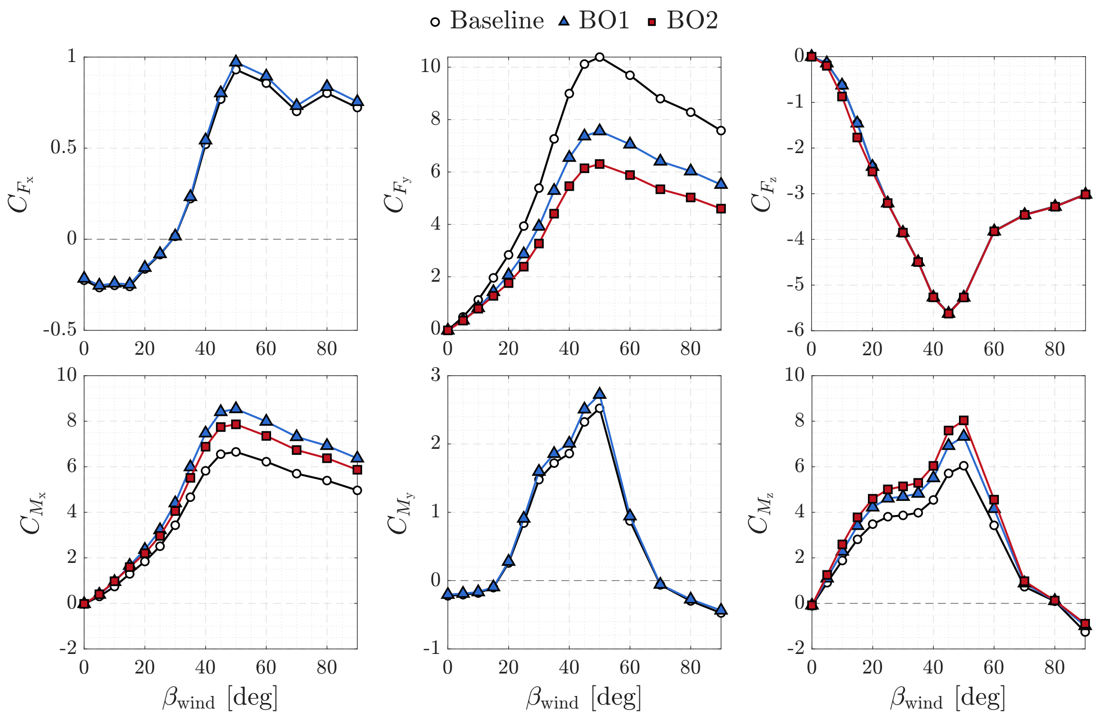

Figure 3: Comparison between baseline (black) and calibrated aerodynamic coefficients. Curves are shown after both the first (blue) and second (red) BO.